

CHAPTER 127

TSUNAMIS SOME LABORATORY AND FIELD OBSERVATIONS

by Fredric Raichlen Assoc Prof of Civil Engineering
W M Keck Laboratory of Hydraulics and Water Resources,
California Institute of Technology, Pasadena, California, U S A

ABSTRACT

A unique laboratory facility to generate waves by impulsive movements of the bottom of a wave tank is described and examples of the wave forms which result are shown. An analytical model is presented for the case of rapid bottom movements which describes, in a qualitative way, certain features of the experiments.

Marigrams from various field stations for the tsunamis from the Chilean earthquake of 1960 and the Alaskan earthquake of 1964 have been analyzed using spectral analysis techniques to determine the harmonic components of these records. Comparisons are made between the spectra of the two tsunamis at each of several locations.

INTRODUCTION

The problems associated with earthquake generated sea waves, known as tsunamis, are serious in many parts of the world particularly around the rim of the Pacific Ocean which is such a seismically active region. Perhaps one of the worst tsunamis of historical times was generated off the coast of Japan on June 15, 1896. The maximum wave which was generated ran up on the near-by land to an elevation of 75 ft to 100 ft above the normal tide level resulting in the death of more than 27,000 persons and the destruction of over 10,000 homes. A much more recent example of the widespread property damage that such a wave system can cause is the tsunami associated with the Alaskan earthquake of March 27, 1964. This tsunami which originated in the Gulf of Alaska caused loss of life and extensive damage as far away as Crescent City California (\$11 million damage). In addition to this distant damage, an estimated \$350 million damage to a number of coastal towns in Alaska could be attributed to the combined effect of the tsunami, soil failure and vibrations.

To learn more about the generation, propagation, and coastal effects of the tsunamis a laboratory study has been initiated which deals with the generation of waves by impulsive bottom movements and the propagation of these waves in the near field. (The near field region is of particular importance to Southern California which appears to be reasonably protected from distant tsunamis, but may be vulnerable to sea waves generated by earthquakes near the coastline.) This investigation is directed toward understanding the phenomenon of bottom generation and the effect of linear and nonlinear dispersion on the resultant wave system. Some preliminary results of the laboratory study are presented herein, thereby demonstrating some of the characteristics and capabilities of the wave generating system which has been developed.

In addition to this laboratory program, field data have been analyzed to gain a better understanding of the interaction of tsunamis with the coastline.

Using spectral analysis techniques certain conclusions can be drawn regarding the effect of the tsunami which resulted from the Alaskan earthquake of 1964 and that resulting from the Chilean earthquake of 1960 on the harbors and embayments where tidal records are available. Hence, this paper is divided into two parts: the first dealing with the laboratory simulation of earthquake generated sea waves and the second dealing with the analysis of field data.

LABORATORY OBSERVATIONS

Experimental Equipment - The experimental program is being conducted in a wave tank which is 31.6 m long, 39 cm wide, and 61 cm deep with glass side-walls throughout. The impulsive wave generator is located at one end of the wave tank and consists, in the initial phases of this study, of a moveable section of the bottom of the wave tank 61 cm long and nearly the same width as the wave tank (39 cm). The section of the bottom can be moved in a pre-determined fashion either upwards or downwards, hence, this system can be thought of as modeling a tectonic movement in nature which is either a simple block upthrust or downthrow. In the laboratory the maximum movement of the bottom in a vertical direction is ± 15 cm with one of the design criterion being that the bottom should be capable of moving ± 3 cm in 0.05 sec. With some modifications the surface area of the generator can be changed.

A schematic drawing of the tsunami generator and the wave tank is presented in Fig. 1. It should be noted that the wave system under investigation is two-dimensional and the rigid wall which exists at $x=0$ represents a plane of symmetry in the true problem. Therefore, with reference to Fig. 1, the total length of the moveable section of the bottom, l , is one-half of the length of the block in nature which is being modeled.

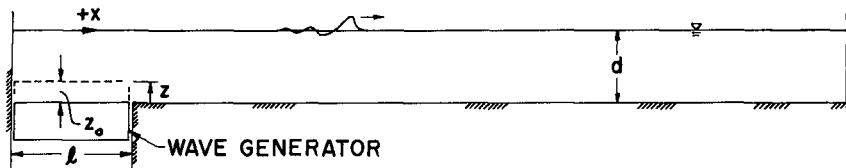


Fig. 1 Schematic Drawing of Impulsive Wave Generator

The wave generator is driven by a hydraulic-servo-system which accepts an input voltage which is proportional to the desired displacement of the bottom, and in this way a variety of bottom motions can be obtained. Basically the system can be divided into three parts: the hydraulic supply unit, the servo-system, and the moveable bed unit assembly.

The hydraulic supply system consisting of oil reservoir, pump, filter, and heat exchange unit supplies the main hydraulic cylinder which actuates the bed with hydraulic fluid at a pressure of 3200 psi. An accumulator is installed in the system primarily to provide a sufficient supply of hydraulic fluid at high pressure to drive the bed for programs which initially demand large flow rates.

The servo-system consists of a servo-valve and its associated electronics used in conjunction with a linear variable differential transformer (LVDT) which senses the motion of the bed. The LVDT with its core mounted to the moving bed and the coil fixed in position provides the electrical feed-back signal which is compared to the input signal supplied by the function generator, by comparing these two signals minor adjustments of the movement of the spool of the servo-valve are made automatically to achieve the desired program of bed movement.

A photograph is presented in Fig. 2 showing in detail the moveable bed unit assembly consisting of the hydraulic cylinder, its supporting structure, two flexures, the load cell, the guide cylinder, the bearing support box, and the bed unit. The hydraulic cylinder which drives the bed is a double-throw type mounted vertically and attached by means of flexures to the laboratory floor and to the bed unit. The flexures provide a means of correcting for any small vertical mis-alignment of the hydraulic cylinder upon installation. The upper flexure is connected to a load cell, for measuring the total applied force, which in turn is connected to the moveable bed unit. The guide cylinder, seen in Fig. 2 moves against two fixed bronze bearings and insures that the bed unit moves in a vertical direction. The bed unit is firmly fixed to the upper surface of the guide cylinder.

Fig. 3 shows the tsunami generator attached to the upstream section of the wave tank with the bed unit in its maximum upward position. A problem in the design of the generator which had to be overcome for successful operation was the sealing of the bed unit around its four sides, two of which are in proximity to glass walls and the other two near machined aluminum surfaces. The seal which was designed and fabricated was a one-piece unit molded of a relatively flexible material and mounted directly to the moveable portion of the bed. Details of this seal can be seen in both Figs. 2 and 3, this type of design (with water on only one side of the generator) minimizes the forces which arise in wave generation.

Some Experimental Results - The time-displacement of the bed which is being used initially is an exponential motion described by the following expression

$$\frac{z}{z_0} = 1 - e^{-\alpha t} \quad (1)$$

where z is the motion of the bed measured positive upwards from the fixed elevation of the bottom of the wave tank, z_0 is the maximum motion of the bed, varying time is represented by t , and α is a coefficient which is equal to the bed velocity divided by the maximum bed displacement, z_0 at $t=0$.

Figs. 4 and 5 are examples of the water surface motions which are generated by such exponential motions of the generator for a water depth of 10 cm and for positive and negative motions respectively. The ratio of the maximum displacement to the depth, z_0/d , for all cases shown was 0.1, and for positive and for negative motions examples are presented for two different non-dimensional times, $t_R(g/d)^{1/2}$, the time t_R is defined as the time that it takes the bed to rise to one-half its maximum value. The two values of the non-dimensional time for which results are shown in Fig. 4 and 5 are $t_R(g/d)^{1/2} = 0.4$ and 3.5 which, for these experiments, correspond to $\alpha = 17.2 \text{ sec}^{-1}$ and 1.96 sec^{-1} respectively. The motion of the bottom is shown as the upper record in each of these figures and is labelled as z .

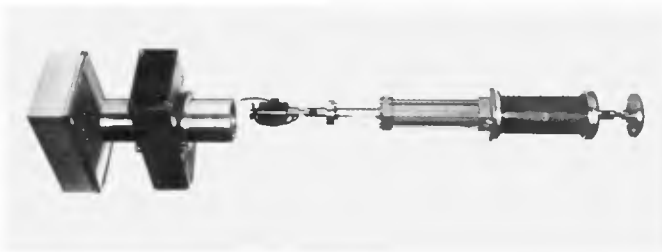


Fig. 2 Exploded View of Moveable
Bed Unit Assembly



Fig. 3 Assembled Impulsive Wave
Generator Attached to Wave Tank

POSITIVE DISPLACEMENT

$$z_0/d = +0.1$$

$$t_R \sqrt{g/d} = 3.5$$

$$t_R \sqrt{g/d} = 0.4$$

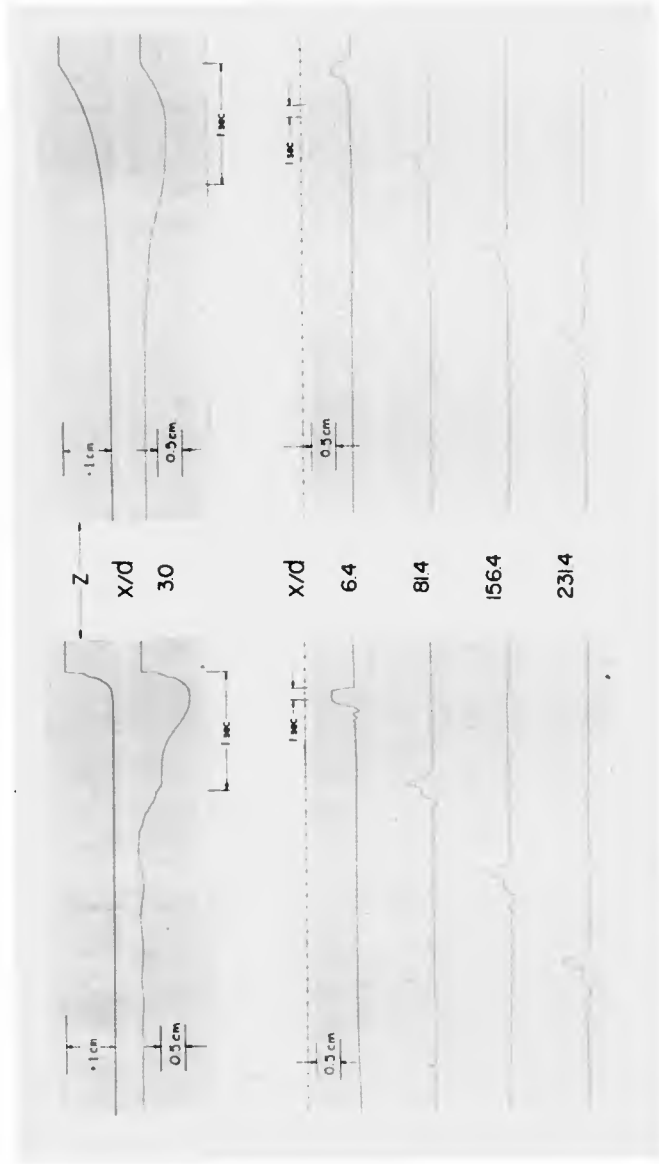


Fig. 4 Oscillograph Records of Bottom Motion and Waves Which Result from a Positive Bottom Displacement, z

NEGATIVE DISPLACEMENT

$Z_0/d = -01$

$t_R \sqrt{g/d} = 0.4$

$t_R \sqrt{g/d} = 3.5$

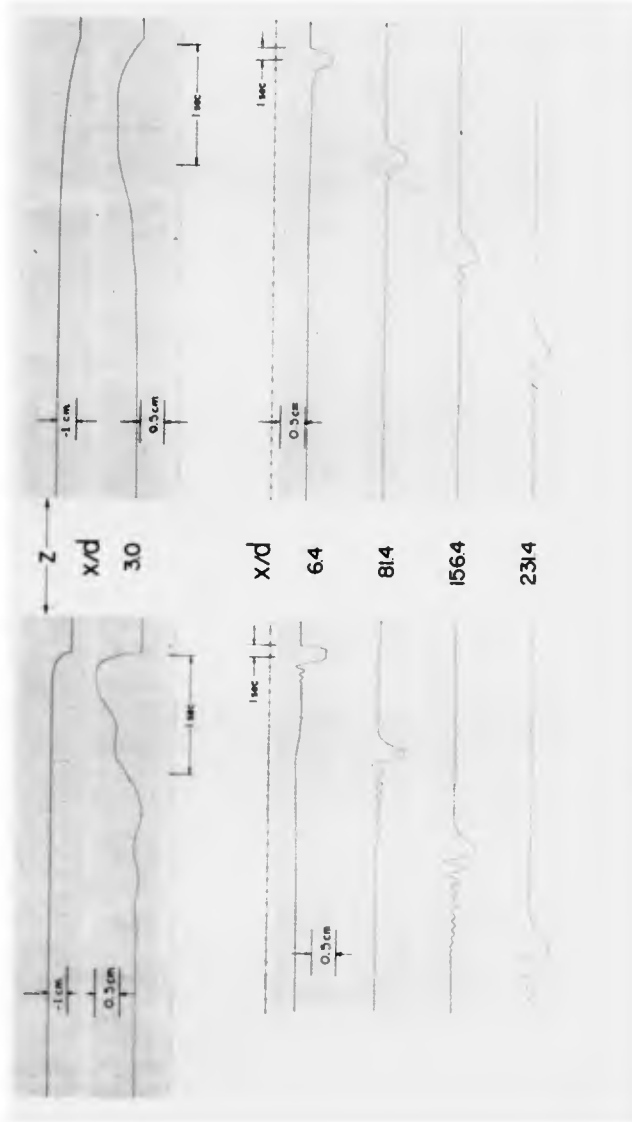


Fig. 5 Oscillograph Records of Bottom Motion and Waves Which Result from a Negative Bottom Displacement, z

In Figs 4 and 5 the variation of the water surface with time measured using resistance wave gages is shown at five different locations along the wave tank. The first location is $x/d = 3.0$ which is approximately midway over the moveable bottom. (Since the wall at $x/d = 0$ also can be thought of as a plane of symmetry for the case of a moving block of length $2l$ centered at $x/d = 0$ for this depth the location $x/d = 3.0$ represents the quarter-point of that moving block, i.e. $x/2l \approx 0.25$.) It should be noted in the oscillograph records which are shown, for the motion of the bottom (z) and for the variation of the water surface at the first location ($x/d = 3.0$) positive movements and water surface displacements are downward at all other locations the positive water surface displacements which are shown on the oscillograph records are upwards. In all of the records time increases to the left, the length of the record which corresponds to one second is indicated in the figure. Four of the wave gages are equally spaced ($x/d = 6.4, 8.1, 15.6, 23.1$) with the first gage located quite close to the "leading edge" of the moving bottom. Since the electronic amplification of the various wave gages has been adjusted to be approximately the same and the gages are equally spaced, a characteristic diagram could be constructed from these four records.

In Fig 4 for the two different non-dimensional times, the upper records show the exponential motion of the bottom. At the location $x/d = 3.0$ for the condition of rapid bottom movement the water surface rises in nearly the same way as does the bottom and begins to fall near the time of maximum bottom displacement. For the experiment with a slower bottom motion the water surface at the same location reaches a maximum before the bottom has fully risen and then begins to fall. For the former case the ratio of the maximum amplitude to the maximum bottom displacement is approximately unity whereas for the latter this ratio is about one-half. Thus, one effect of the magnitude of the non-dimensional time, $t_R(g/d)^{1/2}$, can be seen.

For a non-dimensional time of 0.4, near the edge of the generator ($x/d = 6.4$) the water surface rises quickly to a maximum and remains there for a short period of time before falling. In falling, the water surface elevation first becomes less than the still water level, then rises above the still water level and then oscillates in a damped periodic manner about the quiescent level. As the lead wave progresses downstream it tends to change radically as additional waves are generated from it. In addition to this, groups of waves are evident in the lee of the main wave system and these waves appear to be left further behind in time as the distance from the generation area increases probably due to frequency dispersion.

Similar effects can be seen for the example at a larger non-dimensional time (3.5) except that the dispersive effects are not nearly as pronounced as for the case of the faster bottom movement. Comparing the amplitude of the lead wave for locations $x/d \geq 6.4$ to that at $x/d = 3.0$ it is seen that the waves are approximately 0.8 of the amplitude of the wave over the generator. For the case of a more rapid bottom movement this same ratio was about 0.5 demonstrating another effect of the velocity of the generator on the waves generated.

The comparable case for negative waves is presented in Fig 5. The conditions for the two cases shown are identical to those presented in Fig 4 except a negative motion of $z_0/d = -0.1$ is used. In this case, for the

displacement of the bottom and of the water surface at $x/d = 3.0$ negative displacements are upwards on the oscillograph paper, at all other locations negative displacements are downwards. Comparing the water surface displacements in Figs 4 and 5 at $x/d = 3.0$ and 6.4 for both non-dimensional times it is seen that the negative displacements are nearly mirror images of the positive displacements. However, for a normalized distance of 81.4 major differences are seen between the positive and negative cases. Perhaps the most obvious is the significant growth of a train of waves in the lee of the negative system compared to the positive case which supports the arguments proposed by Keulegan and Patterson (1940) in their paper dealing with non-linear long waves. The effect of dispersion on the lead wave can be seen readily in Fig 5 for the example with the rapid bottom motion from the decrease of the slope of the leading edge of the main wave as the distance from the region of generation increases.

Similar features are evident for the case of a slower bottom movement, $1 \leq t$, a larger non-dimensional time (3.5). Again the features in the lee of the main wave have grown much more rapidly than their positive counterpart. If a comparison is made of the amplitude of the lead wave over the generator to those for $x/d \geq 6.4$, for the case of rapid motion it is found that away from the generator the amplitude is approximately 0.6 of that over the generator. For the slower generator motion this ratio varies from about 0.85 to 0.90. The ratio of the amplitude of the lead wave to the maximum displacement of the generator for the two examples of negative displacements are comparable in magnitude to the corresponding positive cases. Thus, with respect to wave amplitudes there is little difference between the lead wave amplitude resulting from the negative and positive bottom motions for comparable initial conditions.

Some Analytical Considerations - To investigate, in a qualitative sense, some of the features of the wave systems observed in Figs 4 and 5 an analytical method developed by Peregrine (1966) for the treatment of non-linear long waves has been applied. The equations of continuity and momentum can be written in non-dimensional form as

$$\frac{\partial \eta}{\partial t} + \frac{\partial}{\partial x} \left[(1 + \eta) u \right] = 0 \quad (2)$$

$$\frac{\partial u}{\partial t} + u \frac{\partial u}{\partial x} + \frac{\partial \eta}{\partial x} = \frac{1}{3} \frac{\partial^3 u}{\partial x^3 \partial t} + O(\epsilon^2 \sigma^3) \quad (3)$$

All length quantities in Eqs 2 and 3 have been normalized with respect to the depth d , the velocities with respect to the shallow water wave velocity, $(gd)^{1/2}$, and time by multiplying by $(g/d)^{1/2}$. (In the following discussion the same notation as used in Eqs 2 and 3 will be used to denote dimensional and dimensionless quantities; the meaning will be clear from the context of the discussion.) In Eqs 2 and 3 the distance η to the water surface is measured from the still water level, the velocity u is the horizontal velocity averaged over the depth, σ is the ratio of water depth to wavelength, ϵ is the ratio of wave amplitude to water depth, and the notation $O(\)$ indicates terms of the order of the quantity in parentheses and smaller. The solution of these two equations allows for waves traveling in the positive and the negative x -directions, Peregrine's finite difference scheme was used for the numerical solution.

The problem of waves which are formed by an impulsive movement of the bottom was then treated as an initial value problem where the fluid in a long tank is initially at rest everywhere and a mass of fluid is added to (or subtracted

from) the still water surface over a portion of the tank at $t=0$. This theoretical model is crude in the sense that the movement of the bottom is not included instead an assumed form of the water surface is chosen at a time near the end of the wave-maker stroke and before the wave has left the generation area (defined for this analysis as $t=0$). The assumption that the horizontal velocity is initially zero everywhere just when this surface disturbance is formed is probably reasonably close to the experimental conditions for rapid bottom movements. In addition to these features of the analysis, similar to the laboratory conditions, the two ends of the tank in the theory are considered to be solid walls with zero water particle velocity at these walls for all time. This type of initial value problem is similar to that treated by Long (1964) using basically the same expressions as Eqs. 2 and 3 but manipulated in such a way that solutions could be obtained by integrating along the characteristics in the (x, t) plane.

The initial amplitude distribution of the water surface which was used was

$$\frac{\eta}{d} = \pm 0.05 \left[1 - \tanh \left(\frac{x}{d} - 6 \right) \right] \quad (4)$$

From Eq. 4 it is seen that for $x/d < 3$ the amplitude of the water surface is essentially constant and approximately equal to 0.1 and for $x/d > 9$ the amplitude is essentially zero. Such an expression allows for a smooth transition from one water surface elevation to another for the conditions chosen the length of the moveable bed corresponds to $x/d = 6$. With reference to Figs. 4 and 5 it is evident that Eq. 4 compares more favorably with the example which corresponds to the rapid bottom movement. Consider first the amplitude at $x/d = 3$, Eq. 4 gives this amplitude as essentially 0.1 times the depth. In Figs. 4 and 5 the amplitude at this location for the case of rapid motions is approximately the same as the maximum bed motion which is, in relative terms, $z_0/d = \pm 0.1$. From Eq. 4 the relative amplitude at $x/d = 6$ is ± 0.05 which corresponds reasonably well to the observed values of +0.046 and -0.057 at about this location in the experiments for $t_R (g/d)^{1/2} = 0.4$. Thus, although this representation of the water surface is perhaps crude, it does retain some of the important features of the observed distributions.

The analytical results for the case of the positive disturbance are presented in Fig. 6 where the variation in the water surface displacement, η/d is plotted as a function of non-dimensional time $\tau = t(g/d)^{1/2}$, for various values of normalized distance, i.e. $x/d = 0, 3, 10, 20, 30, 40$. A number of interesting features of the problem emerge from this analytical treatment and these will be discussed separately before comparing them to the experimental results. At $x/d = 0$ the wave amplitude decreases with time from the initial value of $\eta/d = 0.1$ to a magnitude less than zero and then oscillates with time about the still water level with the amplitude of oscillation decreasing with time and approaching zero. At $x/d = 10$ the water surface increases gradually with time from zero reaches a maximum, decreases and then increases slightly before decreasing and approaching zero. Hence, a second wave appears to be forming from the lead wave. An additional interesting feature of Fig. 6 is that another group of waves appears in the lee of the main wave for $\tau > 30$. Both of these occurrences is a strong indication of the dispersive nature of such a wave system. For larger values of x/d the main wave appears to begin to move out in front, leaving behind the secondary wave system. If the computer storage had been sufficient to enable the computations to be made for a larger tank and thus to proceed to large values of x/d and τ it might have been possible to see the lead wave approach a solitary wave in form. As it is, because of this limitation the reflection of the wave from the far tank wall can be seen at $x/d = 40$ for $\tau > 80$.

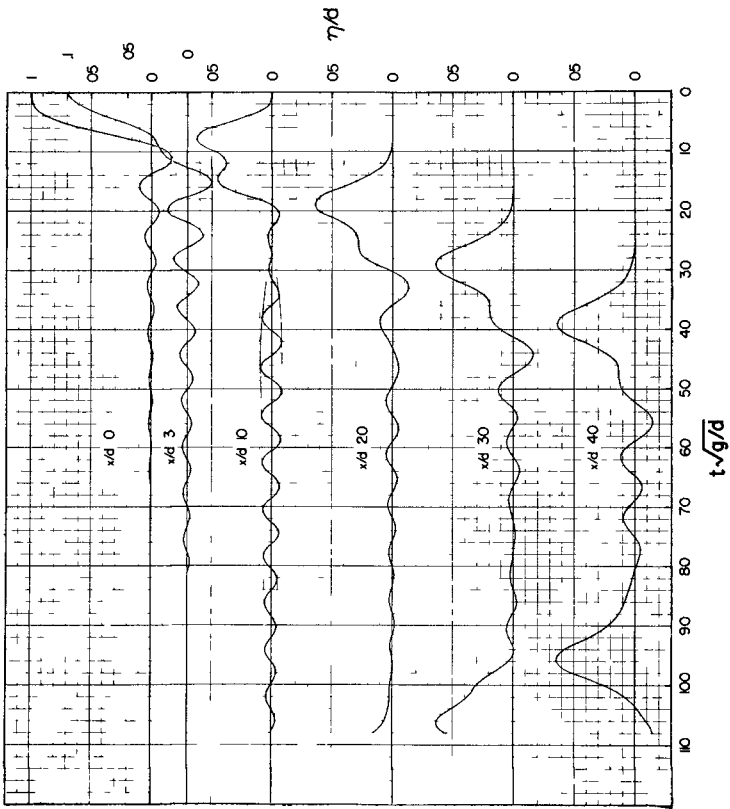


Fig 6 Analytical Results of Waves from a Positive Disturbance

It is interesting to compare Figs 4 and 6 in a qualitative sense. In Fig 4, for either $x/d = 3.0$ or 6.4 the same trailing-edge wave system is observed as at $x/d = 0$ in the analytical solution (Fig 6). The wave systems in both cases decrease to zero with increasing time. Unfortunately, as mentioned previously the analytical solution could not be extended further than $x/d = 40$ so that a station comparable to the next experimental station $x/d = 81.4$ could not be reached. However, in the analytical results similar changes in wave form are observed as in the experiments although perhaps the dispersion occurs more rapidly in the analytical solution than it does in the experiments.

In Fig 7 analytical results are presented for the comparable case of a negative disturbance which propagates from the initial conditions given by Eq 4. At $x/d = 0$ the shape of the disturbance is nearly the mirror image of the positive disturbance shown at the same location in Fig 6, and again trailing waves are seen in the lee of the lead wave. Fig 7 shows that the slope of the leading edge of the main wave decreases with distance as the wave propagates downstream. The same effect is observed when the results are plotted as a function of distance for constant times. If Fig 6 and 7 are compared it is seen that the lead negative disturbance is well formed for a given location compared to the positive wave, and also the trailing waves appear to have grown more rapidly in the case of the negative disturbance compared to the positive one. In addition it has been found that for the last station shown in Fig 7 the variation of the normalized velocity with time is nearly identical to the water surface variation even though at $x/d = 0$ these distributions are different.

If, as before, Fig 7 is compared to its experimental counterpart, Fig 5, the same general trends can be seen: the decreasing slope of the lead wave with distance, the rapid development of the form of the lead wave, and the rapid growth of the waves in the lee of the main disturbance.

In summary, it is felt that this analytical method describes the changes in a wave system due to both linear and nonlinear dispersion. Even though the initial conditions assumed appear crude, the resultant wave forms agree qualitatively with the experiments.

ANALYSIS OF FIELD OBSERVATIONS

In addition to the experimental and analytical studies of which this paper presents only some preliminary results, tide gage records of various tsunamis obtained at certain locations around the Pacific Ocean have been studied to investigate the interaction of these waves with the coastline. An obvious feature of such records is that, even though the particular earthquake has a relatively short duration (of the order of minutes or less), the tide gage records generally exhibit oscillations which last longer than 24 hrs. In addition, the major waves at many of these locations occur within the first few hours of the arrival of the lead wave. An example of such records is presented in Fig 8 for three locations in Southern California for the tsunami which resulted from the Alaskan earthquake of March 27, 1964; these and subsequent records were taken from Spaeth & Berkman (1965) and Berkman & Symons (1964). Such water surface fluctuations at the coastline raise the question whether the wave train which is measured at the coast bears any resemblance to the wave which existed in the open-sea. It is possible that the waves where are recorded are the result of a short impulsive wave train triggering the oscillation of the water masses in local embayments and coastal waters which then oscillate with small damping for long periods of time.

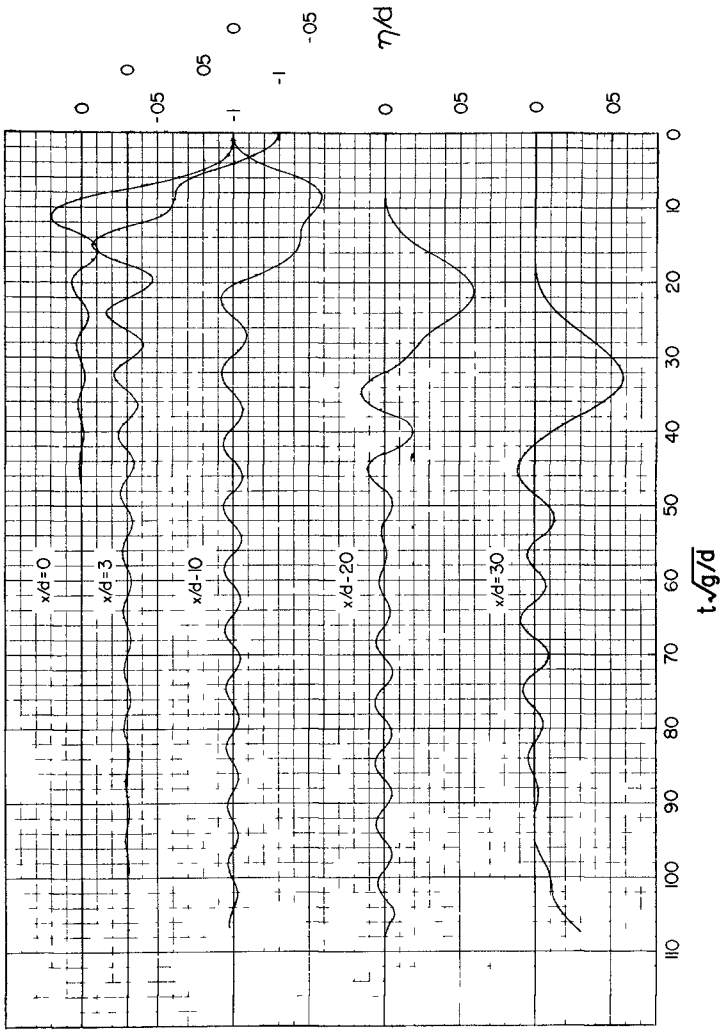


Fig 7 Analytical Results of Waves from a Negative Disturbance

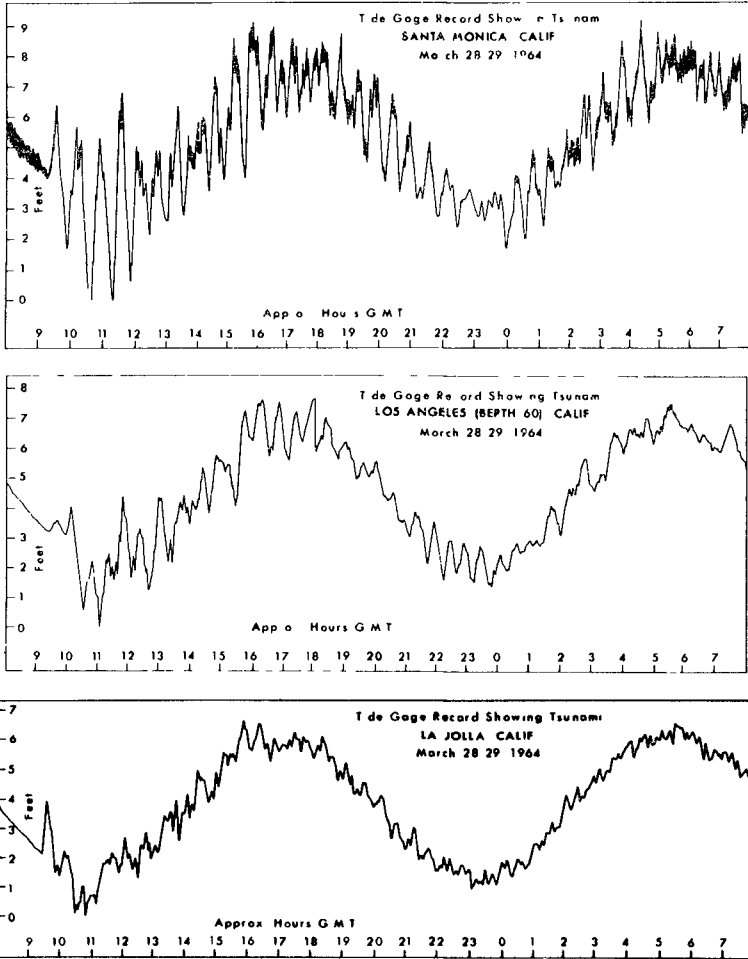


Fig 8 Tide Gage Records from the Tsunami of the Alaskan Earthquake of March 27 1964 (After Spaeth & Berkman (1965))

To investigate this type of question by obtaining information regarding the distribution of wave energy in these records as a function of frequency (or wave period) the wave records were analyzed using spectral analysis procedures similar to those used for analyzing ocean wave records. In essence these methods treat the record as if it were a stationary process. This is not considered too serious a limitation since the primary objective is to compare spectra from various harbors for the same event and from the same harbor for various events, and if approximately the same length of record is treated in the same way for all cases a reasonable comparison can be made. (Of course the same questions regarding stationarity also can be raised about other analytical methods such as harmonic analysis.)

The spectra of the tsunami associated with the Alaskan earthquake of March 27, 1964 for three Southern California locations are presented in Fig. 9. The ordinate in Fig. 9 is the normalized energy density, normalized with respect to the mean square of the deviation of the water surface from the tide level in units of hours and the abscissa is the frequency in cycles per hour (cph). Therefore, the area under each spectrum is unity. The spectra were obtained after subtracting from the marigram the effect of the tide so that this low frequency component would not completely distort the energy content of the spectrum. This was accomplished by first subtracting the predicted or fitted tide from the record and then passing the resultant digitized record through a numerical high-pass filter such as that described by Kinsman (1965). This, as well as the spectral analysis computation was accomplished on a digital computer using the procedure for spectral analysis described by Blackman and Tukey (1958) and by Rachlen (1967). In all cases the confidence limits of the spectra were obtained by applying the method described by Kinsman (1965). For the spectra which are presented it is expected that, for a given frequency-band, if the process were stationary, there is a probability that 90% of all spectral estimates will exceed 0.69 times the ordinate and 10% of all values will exceed 1.30 times the ordinate with 50% of all values exceeding 0.98 times the ordinate value. The frequency resolution which was used was chosen based on the available record lengths, the confidence limits, the sampling interval, and the fact that spectra from different events were to be compared.

Returning now to Fig. 9, spectra are presented for Santa Monica, Los Angeles Harbor (Berth 60) and La Jolla, all in Southern California with the first and last of these locations approximately 125 mi (200 km) apart in a North-South direction. Values of the root-mean-square of the water surface fluctuations about the tide (r_{ms}) are shown in Fig. 9 for these locations. The r_{ms} tends to decrease in a Southerly direction with distance from the tsunami source, in fact, the r_{ms} decreases by a factor of nearly 2.5 comparing the two furthest stations. Considering the problems usually associated with spectral analysis, the spectra for these locations are remarkably similar indicating a major concentration of energy between frequencies of 1.6 cph and 1.8 cph (wave periods between 33.4 min and 37.5 min). In addition, there is a secondary concentration of energy between frequencies of 0.4 cph and 0.6 cph (wave periods between 1.67 hrs and 2.5 hrs). Before discussing in detail some conclusions which may be drawn from these spectra it is useful to view others that have been obtained.

Spectra for four locations are presented in Figs. 10 and 11 for both the tsunami which resulted from the earthquake in Alaska of March 27, 1964 and the earthquake in Chile of May 22, 1960. In all cases the spectra were obtained

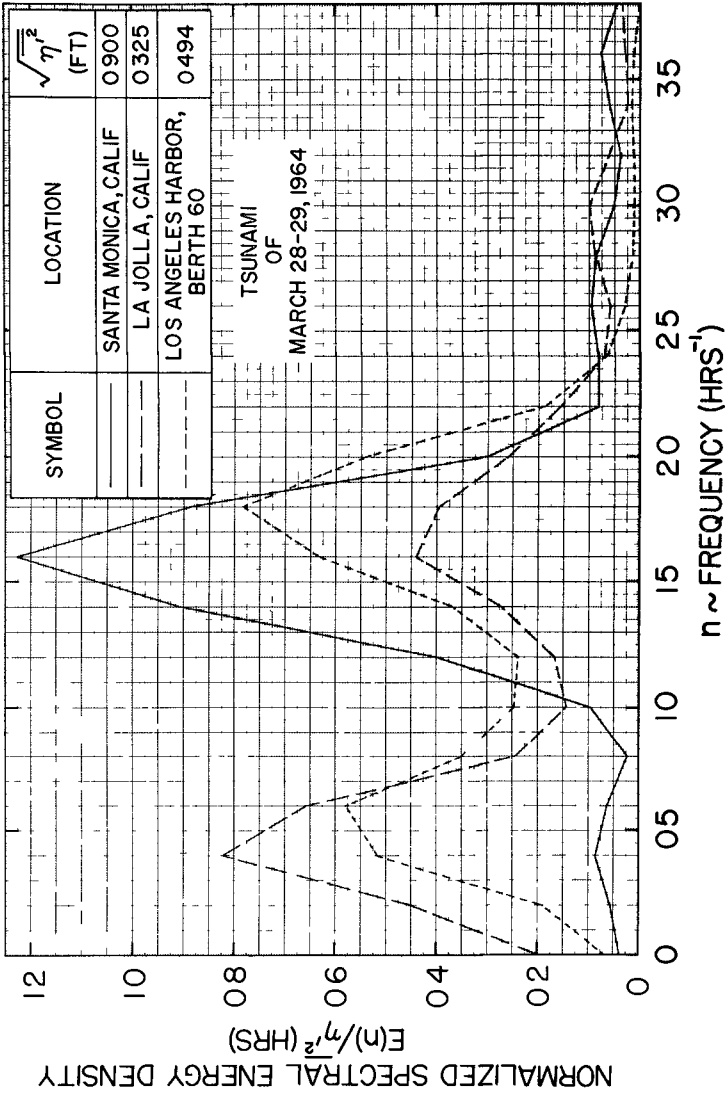


Fig 9 Normalized Energy Spectra for Tsunamis at Three Southern California Locations for the Alaskan Earthquake of March 27 1964

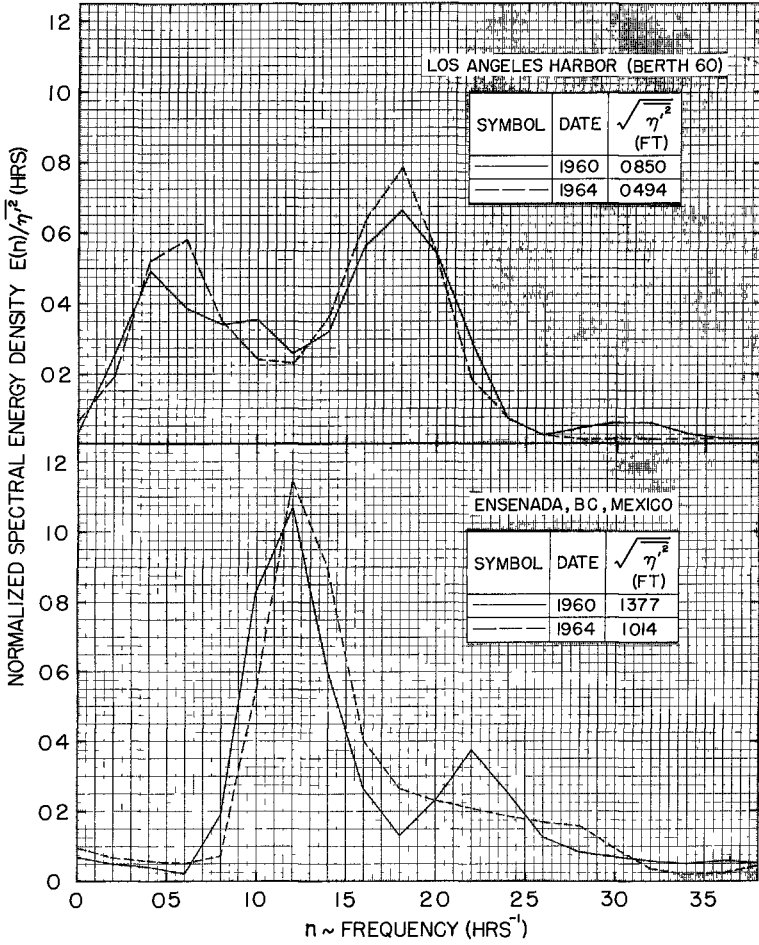


Fig 10 Normalized Energy Spectra for Tsunamis at Los Angeles Harbor (Berth 60) and Ensenada B C , Mexico Caused by Chilean (1960) and Alaskan (1964) Earthquakes

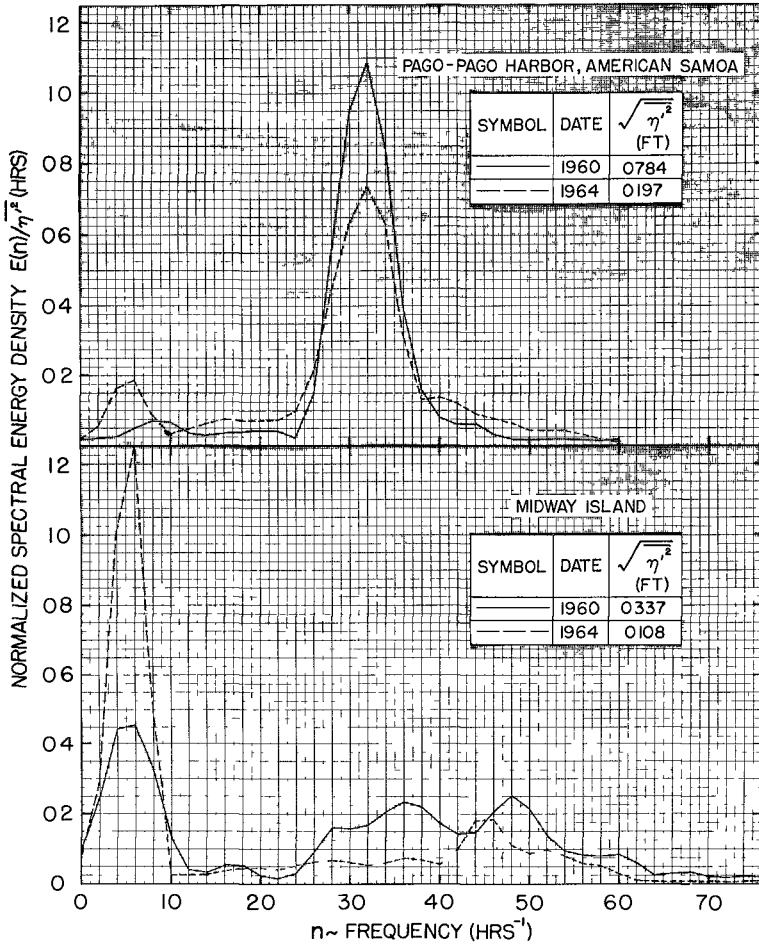


Fig 11 Normalized Energy Spectra for Tsunamis at Pago-Pago Harbor, American Samoa and Midway Island Caused by Chilean (1960) and Alaskan (1964) Earthquakes

and plotted in the same way as those shown in Fig 9 and the values of the $r m s$ are indicated in the figures. There are two obvious features of Figs 10 and 11 (1) the spectra at each location for the two different tsunamis are quite similar, and (2) in all cases the $r m s$ value for the Chilean tsunami is greater than that for the Alaskan tsunami (the ratio varying from nearly 1.4 to 4)

Wilson (1969) in a general investigation of earthquake movements and tsunamis concludes that the tectonic movement associated with both the Chilean earthquake of 1960 and the Alaskan earthquake of 1964 were probably similar and that evidence indicates that a molar upthrust combined with a down-throw played an important role in the earth movement. This similarity may be the reason for the relatively good agreement between spectra at each of the locations shown in Figs 10 and 11. It is also quite possible, as suggested earlier, that each location is very strongly responsive to particular frequencies which are in the tsunami wave train. Therefore, even if the tsunamis were quite different in the open-sea as long as a small amount of energy existed at the preferred frequencies for that particular location, due to the resonant nature of harbors and coastal waters, frequencies to which the harbor is not strongly responsive would be masked. In this way it is possible that spectra at a particular location could be similar even though the spectra of the events in the open-sea were quite different. For the records analyzed it is probable that both of these explanations are true in part, however, from these limited data a more definite conclusion cannot be made.

Wilson (1969) and Munk et al (1959) also have discussed the possibility of the excitation of harbors by these transient wave systems. Munk and Cepeda (1962) have attempted to analyse in some detail the marigram at Acapulco, Mexico due to the tsunami associated with the Mexican earthquake of 1957 to determine whether the response of Acapulco Harbor could be the cause of a sharp peak observed in the spectrum at a frequency of 1.98 cph (a period of about 0.5 hrs). They treated the harbor as if it were a rectangular harbor of constant depth and applied the method of Miles and Munk (1961) to determine the frequencies of various modes of oscillation of this harbor. Their conclusion was that the observed wave period of 0.5 hrs was probably not due to the harbor alone but it was probably caused by the oscillation of a much larger body of water offshore. Their method of determining the response was admittedly crude, and without determining the response by a more exact method such as that developed by Lee (1969) it is difficult to draw a definite conclusion as to the cause of the observed periodicity except to say that the peak which was observed in their spectrum was probably due to local excitations.

Comparing Figs 9, 10, and 11 it is seen that for both tsunamis at three of the four locations investigated there is a peak in all spectra in the period range between 1.67 and 2.5 hrs. (For the Alaskan tsunami alone this periodicity is common to five of the six sites studied.) Ensenada, Mexico is the only location which does not exhibit such a peak, and this may be due to the method of analysis. If the tide is not completely subtracted in the procedure, and if small amounts of energy exist at frequencies near that of the tide, it is possible that the remaining tidal energy can completely mask periodicities with small energy content at low frequencies.

The peaks which are observed in the spectra of Figs 10 and 11 at higher frequencies appear to be common for a particular location, however, these frequencies are not common among locations. Therefore, the energy concentrations which appear at wave periods between 20 min and 50 min are probably due to the bathymetric and coastal configuration of the particular location.

Wilson (1969) and Wilson and Tørum (1968) have concluded that the period of the primary tsunami wave for both the Alaskan tsunami of 1964 and the Chilean tsunami of 1960 was of the order of 1.7 hrs. Since the peaks at the lower frequencies in the spectra presented herein are approximately at the same frequency independent of location, the same conclusion may be made. If one agrees with this conclusion then, considering the periodicity between 33 min and 38 min, Fig 9 indicates that the Alaskan tsunami of 1964 must also have excited a large mass of water off the coast of Southern California extending at least from Santa Monica, California to La Jolla, California. Therefore, in order to learn more about local tsunami effects such as run-up and forces on structures, which are important from engineering considerations, then more must be understood about the response of off-shore water masses to impulsive wave systems.

CONCLUSIONS

The unique laboratory wave generating facility described herein is capable of producing an impulsively generated wave system which shows the same dispersive effects as predicted by a simple theory. The analysis which is used considers the wave system to originate from an initial condition of a disturbed water surface in a still tank of water. It shows, in addition to dispersive effects, the same distinct differences between positive and negative initial disturbances as are observed in the laboratory.

Spectra determined from the tide gage records at four locations around the Pacific Ocean for the tsunamis from the Alaskan earthquake of 1964 and the Chilean earthquake of 1960 had similar shapes at each location. The results indicate that there is a periodicity of approximately 2 hrs which is common to nearly all of the locations investigated. Other concentrations of energy at higher frequencies which for a given location are similar in period for both tsunamis are not similar for different locations. This shows that local embayments and bathymetry tend to influence significantly the wave amplitudes due to tsunamis measured near the shore.

ACKNOWLEDGEMENTS

This research is sponsored by the National Science Foundation under Grant No. GK-2370. The work which deals with the analytical simulation of surface waves was conducted at the Technical University of Denmark while the author was on leave of absence there, the assistance of the Northern Europe University Computing Center in making those computations is appreciated.

REFERENCES

- Berkman S C and Symons, J M "The Tsunami of May 22, 1960 as Recorded at Tide Stations" U S Dept of Commerce, U S Coast and Geodetic Survey, Feb 1964
- Blackman, R B , and Tukey J W , The Measurement of Power Spectra Dover Publications New York N Y , 1958
- Keulegan, G H , and Patterson, G W , "Mathematical Theory of Irrotational Translation Waves", Journal of Research of the National Bureau of Standards Vol 24, Jan 1940, pp 47-101
- Kinsman, B Wind Waves Prentice-Hall, Inc , Englewood Cliffs, New Jersey, 1965, pp 448-455
- Lee, J -J "Wave Induced Oscillations in Harbors of Arbitrary Shape", Report KH-R-20, W M Keck Lab of Hydr & Wat Res , California Institute of Technology Pasadena Calif , Dec 1969
- Long R R "The Initial-Value Problem for Long Waves of Finite Amplitude" Journal of Fluid Mechanics, Vol 20, Part 1, Sept 1964, pp 161-170
- Miles J , and Munk W H , "The Harbor Paradox" Journal of Waterways and Harbors Division, ASCE, Vol 87, No WW3, 1961, pp 111-130
- Munk, W and Cepeda H , "Concerning a Remarkably Sharp Peak in the Sea Level Spectra at Acapulco", Contributions University of California, San Diego, Scripps Institution of Oceanography, Vol 32, 1962 pp 1031-1040
- Munk W H Snodgrass, F E and Tucker, M J , "Spectra of Low Frequency Ocean Waves", Bulln Scripps Instit of Oceanography Vol 7(4), 1959, pp 283-362
- Peregrine, D H , "Calculations of the Development of an Undular Bore", Journal of Fluid Mechanics Vol 25 Part 2 June 1966, pp 321-330
- Rachlen, F , "Some Turbulence Measurements in Water", Journal of the Engineering Mechanics Division, ASCE EM2, Paper 5195, April 1967, pp 78-80
- Spaeth, M B and Berkman, S C , "The Tsunami of March 28, 1964 as Recorded at Tide Stations", U S Dept of Commerce, U S Coast and Geodetic Survey, April 1965
- Wilson, B W "Earthquake Occurrence and Effects in Ocean Areas", Technical Report CR 69 027, prepared for U S N C E L , Port Hueneme, Calif Feb 1969
- Wilson, B W and Tørum, A , "The Alaskan Tsunami of March 1964 Engineering Evaluation", Tech Memo No 25 Coastal Engr Res Cent , Corps Engrs , U S Army, Washington, D C , 1968